Wake effects and energy loss for a charged particle moving above a thin metal film

Chun-Zhi Li,[1,2] Yuan-Hong Song,[1] and You-Nian Wang[1,*]
[1]*School of Physics and Optoelectronic Technology, Dalian University of Technology, Dalian 116023, China*
[2]*College of Physics and Electronic Information, Inner Mongolia University For The Nationalities, Tongliao 028043, China*
(Received 10 April 2009; revised manuscript received 26 May 2009; published 24 June 2009)

We consider a charged particle moving parallel to the surface of a metal film covering on the semi-infinite dielectric substrate with constant speed. By means of the linearized quantum hydrodynamic theory, the induced electron gas density and the stopping power are studied, taking into account the quantum statistical and quantum diffraction effects. The calculation results show that an oscillatory wake field appears apparently behind the particle at both of the surfaces of the metal film and the effect of the film thickness on the electron gas density cannot be neglected when film is thinner. Besides, the dependence of the stopping power on the film thickness, particle position, and the density parameter are analyzed. Finally, the stopping power of our results is compared with those based on the local frequency-dependent dielectric approach.

DOI: 10.1103/PhysRevA.79.062903 PACS number(s): 34.50.Bw, 73.50.−h, 05.60.Gg

I. INTRODUCTION

Electronic excitation, both at the surface and in the bulk of the material, is one of the elementary processes that are well concerned in the field of condensed-matter and surface physics. As is well known, when a charged particle moves near a solid-vacuum interface, an induced potential will be present due to the excitation and polarization of the electrons at the solid surface. The gradient of the induced potential will then give rise to a force that acts back on the moving particle and makes it lose its kinetic energy. Researches on the interaction between charged particles and solid surfaces are not only for electron excitation investigations, but also an effective tool of surface modification or exploration [1,2].

Following the pioneering work of Ritchie [3], there have been many theoretical and experimental methods carried out to study the electron-energy-loss spectroscopy and the wake effects of the interaction between the moving charged particle and solid surface. In particular, Horing [4] investigated the energy loss of a fast particle motion parallel to the two-dimensional (2D) plasma sheet with a fixed distance in the framework of the random-phase approximation (RPA) description within linear-response theory. Apart from RPA theory [5], Wang and Ma [6,7] investigated the wake potential and the energy loss of ions in 2D electron gas by using the local field correction and the quantum scattering theory [8]. Besides, many investigations [9,10] on the energy loss of a charged particle interacting with 2D or three-dimensional electron gas are also carried out by using different methods.

Recently, renewed interest in surface or interface plasmon has attracted more attention in the investigation of the nanostructured materials or electronics at the nanoscale [11]. Especially for the case of thin metal films with certain thicknesses on dielectric substrate, the electric fields of both surfaces interact and make the electron oscillations different from the normal surface plasmon. Researches on thin metal films also show us the strong correlation between the film thickness and film excitation features, such as the dielectric function and the optical constants [12,13], and indicate that selecting the appropriate thickness of a metal film is very important in some film techniques [14]. As we have noticed for the case of the interaction of charged particles and thin films, however, the influence of the film thickness is a question that has not so far received enough theoretical treatment, although it could yield meaningful results for studying more complex systems.

Moreover, the electron gas in ordinary metals is an example of a true quantum plasma that has been studied extensively due to its applications in ultrasmall electronic devices [15], dense astrophysical environments [16], and laser plasmas [17]. The quantum effects become important in plasmas when de Broglie wavelength associated with the particles is comparable to dimension of the system. Among the prevalent models concerning quantum effects in plasma, the quantum hydrodynamic (QHD) [18,19] model has become popular for its extension of the usual fluid model to one incorporating the quantum effects. More recently, this model has been used to investigate dust acoustic solitary waves in quantum plasmas [20] and even the problems in magnetized plasmas [21]. Also based on this model, both the quantum statistical and quantum diffraction effects have been proved to be important in investigating the interactions of charged particles with the quantum electron gas in our previous works [22,23].

In this paper, we employ the linearized QHD theory to study the interaction of the charged particle with a thin metal film located on dielectric substrate. Both the quantum statistical and the quantum diffraction effects are included here, while immobile ions are assumed to form the neutralizing background. The outline of the paper is as follows. In Sec. II, the theoretical model is formulated in terms of QHD equations, cooperated with the Poisson's equation in the appropriate boundary condition, and the analytical expressions of the induced electron gas density and the stopping power are derived. In Sec. III, numerical results are presented and discussed for different parameters, while a comparison of the stopping powers in the QHD model and local frequency-dependent (LFD) dielectric model is provided in Sec. IV. Finally, a short summary is given in Sec. V. Gauss units will be adopted throughout the paper.

*ynwang@dlut.edu.cn

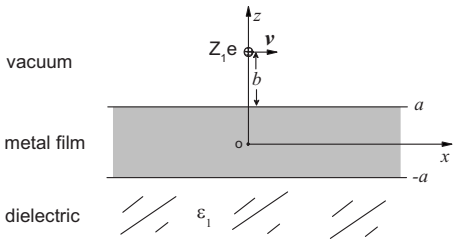

FIG. 1. A charged particle moving with speed v near and parallel to the metal film of thickness $2a$, which covering on the semi-infinite dielectric substrate of relative permittivity ε_1, along the x direction with the height b, the origin of the coordinates is taken at the point of the projection of the moving particle in the $z=0$ plane.

II. THEORETICAL MODEL

We consider a projectile of charge Z_1e flying with constant speed v above a metal film of thickness $2a$, which is covering on the semi-infinite dielectric substrate of relative permittivity ε_1. The schematic diagram is shown in Fig. 1. The metal film lies in the region $|z| \leq a$, with the dielectric substrate located in $z \leq -a$, and the vacuum in $z \geq a$, in a Cartesian coordinate system with $\mathbf{R}=\{\mathbf{r},z\}$. Here, we treat the valence electrons in the metal film as free electron gas immersed in a uniform background of positive charges with the density per unit volume n_0. As the charged particle moves parallel to the metal film along the x axis with a fixed distance b, the homogeneous electron gas will be perturbed by the charged particle $\rho_{ext}=Z_1e\delta(\mathbf{r}-\mathbf{v}t)\delta[z-(a+b)]$ and can be regarded as a charged fluid with three-dimensional scalar density field $n_e(\mathbf{R},t)=n_0+n_{e1}(\mathbf{R},t)$ and a vector velocity field $\mathbf{u}_e(\mathbf{R},t)=\mathbf{u}_{e1}(\mathbf{R},t)$, where $n_{e1}(\mathbf{R},t)$ and $\mathbf{u}_{e1}(\mathbf{R},t)$ represent the first-order perturbed values of the electron gas density and velocity. Based on the linearized QHD theory [18,19], the electronic excitations in the metal film $|z| \leq a$ can be described by the continuity equation

$$\frac{\partial n_{e1}(\mathbf{R},t)}{\partial t} + n_0 \nabla \cdot \mathbf{u}_{e1}(\mathbf{R},t) = 0, \tag{1}$$

the momentum-balance equation

$$m_e \frac{\partial \mathbf{u}_{e1}(\mathbf{R},t)}{\partial t} = e \nabla \Phi_{ind}^{(M)}(\mathbf{R},t) - \frac{m_e\alpha^2}{n_0} \nabla n_{e1}(\mathbf{R},t) + \frac{m_e\beta^2}{n_0} \nabla [\nabla^2 n_{e1}(\mathbf{R},t)] - \gamma m_e \mathbf{u}_{e1}(\mathbf{R},t), \tag{2}$$

and Poisson's equation

$$\nabla^2 \Phi_{ind}^{(M)}(\mathbf{R},t) = 4\pi e n_{e1}(\mathbf{R},t), \tag{3}$$

where m_e is the electron mass, e is the elementary charge, and $\Phi_{ind}^{(M)}$ is the induced potential in the metal film that results from the perturbations of the electron densities. The first term in the right-hand side of Eq. (2) is the force on electron in the metal film due to the electric field. The second term is regarded as the quantum statistical effect caused by the internal interactions in the electrons species. This effect tends to flatten the electron gas density until it reaches the equilibrium state. The third term regarded as quantum diffraction effect comes from the quantum pressure. This effect is the embodiment of wavelike nature of the charge carriers and exists even in a pure quantum-mechanical state, while the last term, $\gamma m_e \mathbf{u}_{e1}(\mathbf{R},t)$, is the frictional force due to the positive charge background, with γ being the frictional coefficient. In particular, $\alpha=\sqrt{3/5}v_F$, $\beta=a_Bv_B/2$, with the Fermi speed $v_F=\hbar(3\pi^2n_0)^{1/3}/m_e$, the Bohr radius $a_B=\hbar^2/e^2m_e$, and the Bohr speed $v_B=e^2/\hbar$, respectively. By eliminating the velocity field $\mathbf{u}_{e1}(\mathbf{r},t)$ in Eqs. (1) and (2), one can obtain

$$\left[\left(\frac{\partial}{\partial t}+\gamma\right)\frac{\partial}{\partial t}\right] n_{e1}(\mathbf{R},t) = -\omega_p^2 n_{e1}(\mathbf{R},t) + \alpha^2\nabla^2 n_{e1}(\mathbf{R},t) - \beta^2\nabla^4 n_{e1}(\mathbf{R},t), \tag{4}$$

where $\omega_p=(4\pi e^2n_0/m_e)^{1/2}$ is the classical plasma frequency in homogeneous electron gas. Then, taking the time-space Fourier transform

$$f(\mathbf{R},t) = \int\int \frac{d\mathbf{k}d\omega}{(2\pi)^3} F(\mathbf{k},z,\omega)e^{i(\mathbf{k}\cdot\mathbf{r}-\omega t)}, \tag{5}$$

here, $\mathbf{k}=k_x\hat{\mathbf{e}}_x+k_y\hat{\mathbf{e}}_y$ is the wave vector in the xoy plane. We expand the perturbed density $n_{e1}(\mathbf{R},t)$ into $n(\mathbf{k},z,\omega)$ according to Eq. (5) and obtain the following expression of Eq. (4):

$$\omega(\omega+i\gamma)n(\mathbf{k},z,\omega) = \omega_p^2 n(\mathbf{k},z,\omega) - \alpha^2\left(-k^2+\frac{d^2}{dz^2}\right)n(\mathbf{k},z,\omega) + \beta^2\left(-k^2+\frac{d^2}{dz^2}\right)^2 n(\mathbf{k},z,\omega). \tag{6}$$

We assume that the expression of $n(\mathbf{k},z,\omega)$ complies with the following form:

$$n(\mathbf{k},z,\omega) = B_+ch(qz) + B_-sh(qz), \tag{7}$$

where sh and ch are the hyperbolic functions and q can be solved from the following equation:

$$\omega(\omega+i\gamma) - \omega_p^2 + \alpha^2(q^2-k^2) - \beta^2(q^2-k^2)^2 = 0. \tag{8}$$

The explicit solution of q will be presented in the Appendix of this paper. Similarly, also by using the Fourier transform in Eq. (5), we expand the induced potential in the metal film $\Phi_{ind}^{(M)}(\mathbf{R},t)$ into $\phi_{ind}^{(M)}(\mathbf{k},z,\omega)$ which has been set as the expression

$$\phi_{ind}^{(M)}(\mathbf{k},z,\omega) = C_+ch(kz) + C_-sh(kz) + D_+ch(qz) + D_-sh(qz). \tag{9}$$

Combining Eqs. (3) and (7) with Eq. (9), we can easily obtain $B_+=(q^2-k^2)D_+/4\pi e$ and $B_-=(q^2-k^2)D_-/4\pi e$.

For the region $z \geq a$, however, the total electric potential is from the external charged particle and the perturbation of the electron fluid density in the metal film, which can be expressed as $\Phi(\mathbf{R},t)=\Phi_{ext}(\mathbf{R},t)+\Phi_{ind}^{(V)}(\mathbf{R},t)$. The induced potential satisfies the Laplace equation, while the external potential obeys the Poisson's equation

$$\nabla^2\Phi_{ext}(\mathbf{R},t) = -4\pi Z_1 e\,\delta(\mathbf{r}-\mathbf{v}t)\,\delta[z-(a+b)], \quad (z \geq a). \tag{10}$$

So, we expand the external potential $\Phi_{ext}(\mathbf{R},t)$ into $\phi_{ext}(\mathbf{k},z,\omega)$ complying with the Fourier expression in Eq. (5), but express the induced potential as

$$\Phi_{ind}^{(V)}(\mathbf{R},t) = \int\int \frac{d\mathbf{k}d\omega}{(2\pi)^3} A(\mathbf{k},\omega) e^{i(\mathbf{k}\cdot\mathbf{r}-\omega t)-kz}. \tag{11}$$

For the region $z \leq -a$, the induced potential can be similarly expanded as

$$\Phi_{ind}^{(D)}(\mathbf{R},t) = \int\int \frac{d\mathbf{k}d\omega}{(2\pi)^3} D(\mathbf{k},\omega) e^{i(\mathbf{k}\cdot\mathbf{r}-\omega t)+kz}. \tag{12}$$

The coefficients $A(\mathbf{k},\omega)$, $D(\mathbf{k},\omega)$, C_+, C_-, D_+, and D_- in the above equations are to be determined from the matching boundary conditions of the fields at $z=\pm a$.

As the electron gas is confined in the metal film, the component of $\mathbf{u}_{e1}(\mathbf{R},t)$ normal to the surfaces is zero, i.e., $u_{e1}(\mathbf{k},z,\omega)|_{z=\pm a}=0$; here, the detailed expression of $u_{e1}(\mathbf{k},z,\omega)$ can be obtained from Eqs. (2) and (5). Furthermore, we adopt the boundary conditions of the potential and the normal component of electronic displacement at $z=\pm a$, as

$$[\phi_{ext}(\mathbf{k},z,\omega) + A(\mathbf{k},\omega)e^{-kz}]|_{z=a} = \phi_{ind}^{(M)}(\mathbf{k},z,\omega)|_{z=a},$$

$$D(\mathbf{k},\omega)e^{kz}|_{z=-a} = \phi_{ind}^{(M)}(\mathbf{k},z,\omega)|_{z=-a}, \tag{13}$$

and

$$\frac{\partial}{\partial z}[\phi_{ext}(\mathbf{k},z,\omega) + A(\mathbf{k},\omega)e^{-kz}]|_{z=a} = \frac{\partial}{\partial z}\phi_{ind}^{(M)}(\mathbf{k},z,\omega)|_{z=a},$$

$$\varepsilon_1\frac{\partial}{\partial z}D(\mathbf{k},\omega)e^{kz}|_{z=-a} = \frac{\partial}{\partial z}\phi_{ind}^{(M)}(\mathbf{k},z,\omega)|_{z=-a}. \tag{14}$$

We can obtain the expressions of the coefficients

$$A(\mathbf{k},\omega) = e^{ka}\left[\frac{PC_+ + QC_-}{q\omega(\omega+i\gamma)} - \phi_{ext}(\mathbf{k},a)\right], \tag{15}$$

$$D(\mathbf{k},\omega) = e^{ka}\left[\frac{PC_+ - QC_-}{q\omega(\omega+i\gamma)}\right], \tag{16}$$

$$C_+ = 2q\omega(\omega+i\gamma)\frac{\varepsilon_1 Q + qT}{(P+qS)(\varepsilon_1 Q+qT)+(Q+qT)(\varepsilon_1 P+qS)} \times \phi_{ext}(\mathbf{k},a), \tag{17}$$

$$C_- = 2q\omega(\omega+i\gamma)\frac{\varepsilon_1 P + qS}{(P+qS)(\varepsilon_1 Q+qT)+(Q+qT)(\varepsilon_1 P+qS)} \times \phi_{ext}(\mathbf{k},a), \tag{18}$$

$$D_+ = -\frac{\omega_p^2}{\omega(\omega+i\gamma)}\frac{k}{q}\frac{sh(ka)}{sh(qa)}, \tag{19}$$

and

$$D_- = -\frac{\omega_p^2}{\omega(\omega+i\gamma)}\frac{k}{q}\frac{ch(ka)}{ch(qa)}, \tag{20}$$

where $P=q\omega(\omega+i\gamma)ch(ka)-k\omega_p^2 sh(ka)cth(qa)$, $Q=q\omega(\omega+i\gamma)sh(ka)-k\omega_p^2 ch(ka)th(qa)$, $S=[\omega(\omega+i\gamma)-\omega_p^2]sh(ka)$, $T=[\omega(\omega+i\gamma)-\omega_p^2]ch(ka)$, and $\phi_{ext}(\mathbf{k},a)=\frac{8\pi^2 Z_1 e}{k}e^{-kb}\delta(\omega-\mathbf{k}\cdot\mathbf{v})$. So we can calculate the spatial distribution of the induced electron gas density in the metal film from Eq. (7) by using the inverse Fourier transform and the above expressions of the coefficients.

Furthermore, we study here the stopping powers that represent the main effects of the induced electric field on a charged particle moving above the metal film. Using the expression for the induced potential given in Eq. (11) and combining it with Eq. (15), the stopping power can be described as follows:

$$S = Z_1 e\left.\frac{\mathbf{v}\cdot\nabla\Phi_{ind}^{(V)}}{v}\right|_{\mathbf{r}=\mathbf{v}t,z=(a+b)} = \frac{Z_1 e}{v}\int\int\frac{d\mathbf{k}d\omega}{(2\pi)^3} i\mathbf{k}\cdot\mathbf{v}\mathbf{A}(\mathbf{k},\omega)e^{i(\mathbf{k}\cdot\mathbf{r}-\omega t)-k(a+b)}. \tag{21}$$

In this paper, we take $\mathbf{k}\cdot\mathbf{v}=k_x v=\omega$ due to the assumption of the charged particle moving along the x axis. Moreover, it is convenient for calculation to introduce the dimensionless variables $v/v_B \to v$, $\omega/\omega_p \to \omega$, $l/\lambda_F \to l$, $\gamma/\omega_p \to \gamma$, and $k/k_F \to k$, where l stands for any quantity of length. Besides, $k_F=(3\pi^2 n_0)^{1/3}$ is the Fermi wave number, $\lambda_F=1/k_F$ is the Fermi wavelength, and $r_s=(3/4\pi a_B^3 n_0)^{1/3}$ is a dimensionless parameter that has been introduced to represent the electron gas density in equilibrium.

III. NUMERICAL RESULTS

In our calculation, we take the charged particle as a proton, $Z_1=1$, and the relative permittivity $\varepsilon_1=3.0$. Figures 2(a) and 2(b) show the spatial distribution of the induced electron gas density [normalized by $n_{e0}=(\sqrt{3}\pi^{5/2}a_B^3)^{-1}$] in the metal film along the z and x directions for different film thicknesses: (a) $a=6\lambda_F$ and (b) $15\lambda_F$, with the particle speed $v=3v_B$. It is found from the figures that a kind of oscillatory wake field appears apparently behind the particle position ($x=0$) along the x direction. The oscillatory state of the electron gas density in the vicinity of the upper surface ($z=a$) is almost invariant with the increase in the film thickness. Along the z direction, however, one can see from Fig. 2(a) that the oscillatory amplitude decreases and almost disappears at first, and then begins to increase near the lower surface of the film ($z=-a$). This characteristic may be due to the limitation of the film thickness, which therefore makes the electrons accumulate at the lower surface. Besides, one can see from Fig. 2(b), the oscillation near the lower surface gradually disappears with the increasing film thickness and the electron density perturbation will no longer put any effects as the film thickness increases up to a certain value. Thus, from our results, the influence of the induced electron gas densities due to the intrusive proton cannot be neglected at the metal-dielectric interface as the metal film is relative

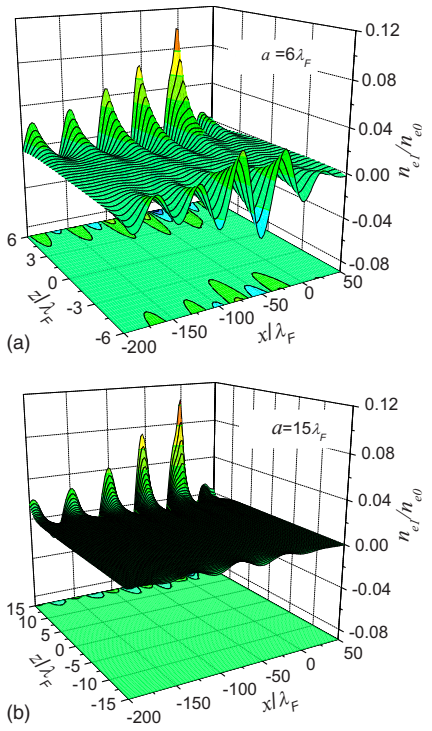

FIG. 2. (Color online) The distribution of the induced electron gas density n_{e1} [normalized by $n_{e0}=(\sqrt{3}\pi^{5/2}a_B^3)^{-1}$] along the x and z directions in the metal film for different film thicknesses: (a) $a=6\lambda_F$, and (b) $15\lambda_F$ with $\gamma=0.05\omega_p$, $r_s=3$, and $b=3\lambda_F$. The solid line in the xoz plane is the projection of the n_{e1}.

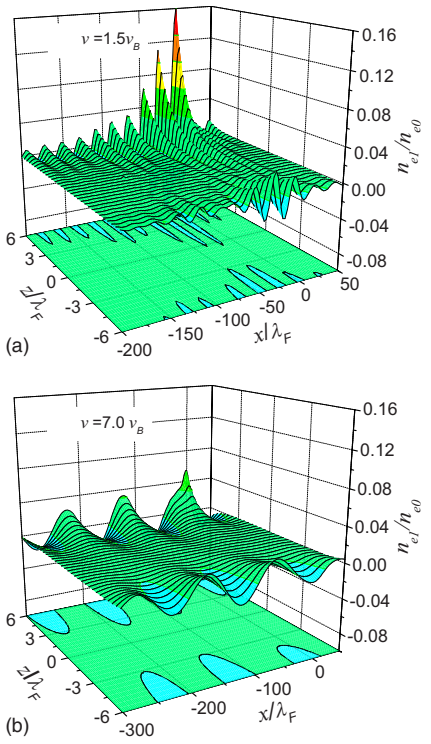

FIG. 3. (Color online) The distribution of the normalized induced electron gas density along x and z directions for different particle speeds: (a) $v=1.5v_B$, and (b) $v=7v_B$ with $\gamma=0.05\omega_p$, $r_s=3$, and $b=3\lambda_F$.

thin. But, the depth of this kind of influence is finite in a given case when the thickness is up to a certain value.

To examine the effects of the particle speed on the perturbation of the electron gas, in Figs. 3(a) and 3(b), we plot the spatial distribution of the induced density in xoz plane for different particle speeds: (a) $v=1.5v_B$, and (b) $v=7v_B$, with $a=6\lambda_F$. For a particular value of particle speed, similar to what Fig. 2 shows, an oscillatory wake field excited behind the test charge and the cumulative electrons exist near the lower surface of the film. However, with the increasing particle speed v, the maximum amplitude of the oscillation reduces and the wavelength becomes longer. Besides, longer tails of the wake effects behind the proton at both of the surfaces of the metal film are noticed as the particle speed v increases.

Stopping powers dependent on the thickness of the metal film a, the height of the particle b, and the density parameter r_s are shown in Fig. 4, with $\varepsilon_1=3$ and $\gamma=0.1\omega_p$. Figure 4(a) displays the stopping power as a function of particle speed for different film thickness, with $b=3\lambda_F$ and $r_s=3.0$. From the figure one can see that the energy loss of the particle is hardly influenced by the thickness of the metal film when the particle speed is lower than $v\simeq 2$ at which the stopping powers take the maximum value. However, at the speed much higher than $v\simeq 2$, the stopping powers for thicker films are greater than the case for $a=5\lambda_F$ but will not increase too much as the film thickness still increases. The effects of the particle position on the stopping powers are shown in Fig. 4(b). Similar to our work [22] in which the interaction of moving charged particle with two-dimensional electron gas is discussed, the stopping power increases in magnitude with the decreasing b value and the extrema in curves shift toward the lower velocity indicating more energy will be lost when the particle moves closer to the metal film. Figure 4(c) shows us the influences of different metal films on the stopping powers, in which one can see that the stopping power increases in a higher speed region with the decreasing r_s, showing that stronger excitation and polarization will happen in the electron gas with higher densities.

IV. COMPARISON WITH LFD DIELECTRIC APPROACH

In this section, we try to recalculate the stopping power of protons by using the LFD dielectric function to describe the collective response of the electron in the metal film instead of the QHD model. The expression of the dielectric function is

$$\varepsilon(\omega) = 1 - \frac{\omega_p}{\omega(\omega + i\gamma)}, \tag{22}$$

where ω_p is the classical plasma frequency and γ is the frictional coefficient, same as those in Eq. (4). We assume that the potential in the metal film can be described as

$$\Phi^{(M)}(\mathbf{R},t) = \int\int \frac{d\mathbf{k}d\omega}{(2\pi)^3}[Be^{-kz} + Ce^{kz}]e^{i(\mathbf{k}\cdot\mathbf{r}-\omega t)}. \tag{23}$$

Thus the boundary conditions in Eqs. (13) and (14) will be changed into

$$\phi_{ext}(\mathbf{k},a) + A(\mathbf{k},\omega)e^{-ka} = Be^{-ka} + Ce^{ka},$$

$$Be^{ka} + Ce^{-ka} = De^{-ka}, \tag{24}$$

and

$$\phi_{ext}(\mathbf{k},a) - A(\mathbf{k},\omega)e^{-ka} = -\varepsilon(\omega)[Be^{-ka} - Ce^{ka}],$$

$$-\varepsilon(\omega)[Be^{ka} - Ce^{-ka}] = \varepsilon_1 De^{-ka}. \tag{25}$$

Substituting Eq. (22) into the boundary conditions Eqs. (24) and (25), we finally obtain

$$A(\mathbf{k},\omega) = \frac{\varepsilon(\omega)ch(2ka) + \varepsilon_1 sh(2ka) - \varepsilon(\omega)[\varepsilon(\omega)sh(2ka) + \varepsilon_1 ch(2ka)]}{\varepsilon(\omega)ch(2ka) + \varepsilon_1 sh(2ka) + \varepsilon(\omega)[\varepsilon(\omega)sh(2ka) + \varepsilon_1 ch(2ka)]} e^{ka}\phi_{ext}(\mathbf{k},a), \tag{26}$$

which is to be used in Eq. (21) to evaluate the stopping power in the LFD dielectric function approach. In Fig. 5, we calculate the stopping powers in this approach and compare them with those obtained from QHD theory, for particles moving above the metal film at different position b, with $a=10\lambda_F$, $r_s=2$, $\gamma=0.1\omega_p$, and $\varepsilon_1=3$. From the figure one can see that two groups of results coming from different theoretical models appear to be close for high speed indicating that the LFD dielectric approach may be considered as a simple approximation to the QHD model when the particle speed is high. For the large distance like $b=20\lambda_F$, the values of stopping power calculated from two models are almost in agreement with each other independent of proton speed. But, for the case of particles close to the film or those with low speed, the results based on the LFD dielectric approach seem to overestimate the stopping values compared with those in the QHD model.

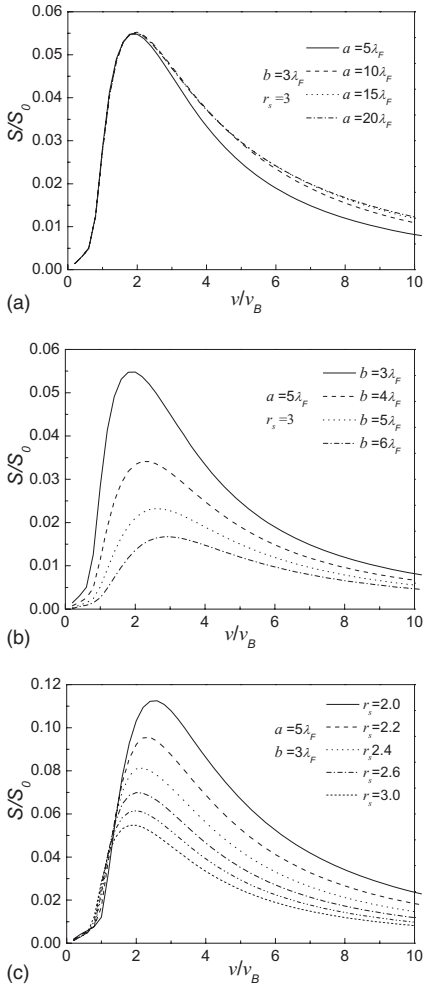

FIG. 4. The stopping power S [normalized by $S_0=(2Z_1e/\sqrt{3}\pi a_B)^2$] versus the moving particle speed v (normalized by v_B) for different thickness a, with $b=3\lambda_F$, and $r_s=3$ (a), for different particle position b, with $a=5\lambda_F$, and $r_s=3$ (b), and for different density parameter r_s, with $a=5\lambda_F$ and $b=3\lambda_F$ (c).

V. SUMMARY

This work presents a theoretical description of the interaction of a moving charged particle with the thin metal film covering on the semi-infinite dielectric substrate based on the QHD model. The analytical expressions of the induced electron density and the stopping power have been derived with the assumption of the linear disturbance. The simulation results indicate that the oscillatory wake effects occur behind the particle opposite to the particle motion when the particle moves above the metal film. The oscillatory behavior turns up near both of the surfaces of the metal films with limited thickness and the wake effects at the lower surface will dis-

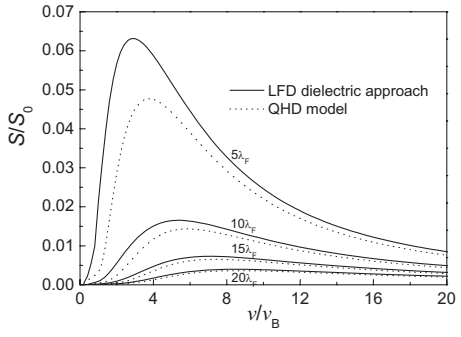

FIG. 5. Stopping power S (multiplied by distance b) vs particle speed v for distances $b=5$, 10, 15, and $20\lambda_F$ from the metal surface. The solid curves are the results of the LFD model and the dotted curves are the results of QHD dielectric approach, with $a=10\lambda_F$, $r_s=2$, $\gamma=0.1\omega_p$, and $\varepsilon_1=3$.

appear with the increase in the film thickness indicating that the film thickness has important influence on the induced density especially at the metal-dielectric interface. Also, comparing the results from different particle speeds, the particle with higher speed can stimulate wake effects with longer tails and will face weaker damping at both of the surfaces. Moreover, as a function of the particle speed, the stopping powers dependent on the thickness of the metal film, the height of the particle, and the density parameter have been discussed. Our calculation results indicate that the stopping power weakly relies on the film thickness in the low velocity region but increases with the increase in thickness a in a higher region, until a is up to a certain value. In addition, smaller distance from the metal surface and greater density of the electron gas will both lead to stronger wake effects and then stronger stopping to the intruding particle. From comparisons of the stopping powers in the QHD model with those based on the LFD dielectric function model, we find that our calculation results in this work are capable to be relied on. For our future study, we would like to extend the present work to investigate the interactions of ions or laser beam with metal films.

ACKNOWLEDGMENTS

This work was supported by National Natural Science Foundation of China (Y.N.W., Grant No. 10635010) and Program for New Century Excellent Talents in University (Y.H.S., Grant No. NCET-08-0073).

APPENDIX

We know from the paper that q can be solved from the following equation:

$$\omega(\omega + i\gamma) - \omega_p^2 + \alpha^2(q^2 - k^2) - \beta^2(q^2 - k^2)^2 = 0. \quad \text{(A1)}$$

Thus, the expression of q^2 can be given as

$$q^2 = k^2 + \frac{\alpha^2}{2\beta^2} \pm \frac{\alpha^2}{2\beta^2}\left\{1 + \frac{4\beta^2}{\alpha^4}[\omega(\omega + i\gamma) - \omega_p^2]\right\}^{1/2}. \quad \text{(A2)}$$

For the momentum-balance equation in Eq. (2), the term $\frac{\beta^2}{n_0}\nabla[\nabla^2 n_{e1}(\mathbf{R},t)]$ is the quantum diffraction effect coming from the quantum pressure, which is very small compared to the electric-field force and the quantum statistical effects. Therefore, if $\beta \to 0$, the solution of q^2 should be consistent with that coming from the following equation:

$$\frac{\partial \mathbf{u}_{e1}(\mathbf{R},t)}{\partial t} = \frac{e}{m_e}\nabla \Phi_{ind}^{(M)}(\mathbf{R},t) - \frac{\alpha^2}{n_0}\nabla n_{e1}(\mathbf{R},t) - \gamma \mathbf{u}_{e1}(\mathbf{R},t), \quad \text{(A3)}$$

i.e.,

$$q^2 = k^2 + \frac{1}{\alpha^2}[\omega_p^2 - \omega(\omega + i\gamma)]. \quad \text{(A4)}$$

When $\beta \to 0$, the third term on the right-hand side of Eq. (A2) will close to

$$\frac{\alpha^2}{2\beta^2} - \frac{1}{\alpha^2}[\omega_p^2 - \omega(\omega + i\gamma)]. \quad \text{(A5)}$$

So, only when we take the symbol "–" in Eq. (A2) is the expression of which consistent with that of Eq. (A4).

[1] E. Taglauer, Surf. Sci. **299-300**, 64 (1994).
[2] A. Gupta, Vacuum **58**, 16 (2000).
[3] R. H. Ritchie, Phys. Rev. **106**, 874 (1957).
[4] N. J. M. Horing, H. C. Tso, and G. Gumbs, Phys. Rev. B **36**, 1588 (1987).
[5] A. Bergara, I. Nagy, and P. M. Echenique, Phys. Rev. B **55**, 12864 (1997).
[6] Y. N. Wang and T. C. Ma, Phys. Rev. B **52**, 16395 (1995).
[7] Y. N. Wang and T. C. Ma, Phys. Lett. A **200**, 319 (1995).
[8] Y. N. Wang and T. C. Ma, Phys. Rev. A **55**, 2087 (1997).
[9] K. Tőkési, X. M. Tong, C. Lemell, and J. Burgdörfer, Phys. Rev. A **72**, 022901 (2005).
[10] J. Osma and F. J. García de Abajo, Phys. Rev. A **56**, 2032 (1997).
[11] J. M. Pitarke, V. M. Silkin, E. V. Chulkov, and P. M. Echenique, Rep. Prog. Phys. **70**, 1 (2007).
[12] G. K. Pribil, B. Johs, and N. J. Ianno, Thin Solid Films **455-456**, 443 (2004).
[13] J. N. Hilfiker *et al.*, Thin Solid Films **516**, 7979 (2008).
[14] V. S. Kovivchak, R. B. Burlakov, T. V. Panova, and N. A. Davletkil'deev, Tech. Phys. Lett. **34**, 358 (2008).
[15] P. A. Markowich, C. Ringhofer, and C. Schmeiser, *Semiconductor Equations* (Springer, Vienna, 1990).
[16] Y. D. Jung, Phys. Plasmas **8**, 3842 (2001).
[17] D. Kremp, T. Bornath, M. Bonitz, and M. Schlanges, Phys. Rev. E **60**, 4725 (1999).
[18] F. Haas, G. Manfredi, and M. Feix, Phys. Rev. E **62**, 2763 (2000).
[19] G. Manfredi and F. Haas, Phys. Rev. B **64**, 075316 (2001).
[20] S. Ali and P. Shukla, Phys. Plasmas **13**, 022313 (2006).
[21] F. Haas, Phys. Plasmas **12**, 062117 (2005).
[22] C. Z. Li, Y. H. Song, and Y. N. Wang, Phys. Lett. A **372**, 4500 (2008).
[23] C. Z. Li, Y. H. Song, and Y. N. Wang, Chin. Phys. Lett. **25**, 2981 (2008).